SECURITY CLASSIFICATION OF THIS PAGE

REPORT DOCUMENTATION PAGE

AD-A242 445

DTIC ELECTE DEC 8 1991 C D

1b. RESTRICTIVE MARKINGS	
2b. DECLASSIFICATION / DOWNGRADING SCHEDULE	3. DISTRIBUTION / AVAILABILITY OF REPORT: **Unclassified/Unlimited**
4. PERFORMING ORGANIZATION REPORT NUMBER(S): **ONR Technical Report 5**	5. MONITORING ORGANIZATION REPORT NUMBER(S)
6a. NAME OF PERFORMING ORGANIZATION: **Dept of Chemical Engineering and Materials Science** / 6b. OFFICE SYMBOL (If applicable): **Code 1113**	7a. NAME OF MONITORING ORGANIZATION: **Office of Naval Research**
6c. ADDRESS (City, State, and ZIP Code): **University of Minnesota Minneapolis, MN 55455**	7b. ADDRESS (City, State, and ZIP Code): **800 North Quincy Street Arlington, VA 22217**
8a. NAME OF FUNDING / SPONSORING ORGANIZATION: **Office of Naval Research** / 8b. OFFICE SYMBOL (If applicable)	9. PROCUREMENT INSTRUMENT IDENTIFICATION NUMBER: Contract No. N00014 91-J-1927
8c. ADDRESS (City, State, and ZIP Code): **800 North Quincy Street Arlington, VA 22217-5000**	10. SOURCE OF FUNDING NUMBERS: PROGRAM ELEMENT NO. / PROJECT NO. / TASK NO. / WORK UNIT ACCESSION NO

11. TITLE (Include Security Classification)
A Scanning Tunneling Microscopy Investigation of the Annealing of the Au(III) Surface

12. PERSONAL AUTHOR(S)
Shelly R. Snyder

13a. TYPE OF REPORT	13b. TIME COVERED	14. DATE OF REPORT (Year, Month, Day)	15. PAGE COUNT
Technical	FROM 1/1/91 TO 10/31/93	November 10, 1991	17 pages

16. SUPPLEMENTARY NOTATION
submitted to the Journal of the Electrochemical Society

17. COSATI CODES		
FIELD	GROUP	SUB-GROUP

18. SUBJECT TERMS (Continue on reverse if necessary and identify by block number)
STM, Au(111), Surface reconstruction

19. ABSTRACT (Continue on reverse if necessary and identify by block number)

This report describes how the quenching and annealing procedure can affect the formation and morphology of Au(111) facets. We show that elastic and plastic deformations that occur in the Au sphere upon rapid cooling can propagate across the facet to produce highly-ordered surface features with corrugation amplitudes of ~2-12Å and a periodicity of ~60Å superimposed on atomically flat terraces. The effects of annealing the Au sphere on this structure and the appearance of the $\sqrt{3}$ x 22 surface reconstruction of Au(111) are discussed

20. DISTRIBUTION / AVAILABILITY OF ABSTRACT	21. ABSTRACT SECURITY CLASSIFICATION
☒ UNCLASSIFIED/UNLIMITED ☐ SAME AS RPT ☐ DTIC USERS	**Unclassified**
22a. NAME OF RESPONSIBLE INDIVIDUAL: **Henry S. White**	22b. TELEPHONE (Include Area Code): **(612) 625-6345** / 22c. OFFICE SYMBOL

DD FORM 1473, 84 MAR — 83 APR edition may be used until exhausted. All other editions are obsolete.

SECURITY CLASSIFICATION OF THIS PAGE

OFFICE OF NAVAL RESEARCH

Contract N00014-91-J-1927

R&T Code 413v001

Technical Report No. 5

A SCANNING TUNNELING MICROSCOPY INVESTIGATION OF THE ANNEALING OF THE Au(111) SURFACE

by

SHELLY R. SNYDER

Prepared for Publication in the

JOURNAL OF THE ELECTROCHEMICAL SOCIETY

University of Minnesota
Department of Chemical Engineering and Materials Science
Minneapolis, MN 55455

November 10, 1991

ECS Summer Fellowship Report
→to be published in the Journal of the Electrochemical Society

A Scanning Tunneling Microscopy Investigation of the Annealing of the Au(111) Surface

Shelly R. Snyder
Department of Chemical Engineering and Materials Science
University of Minnesota
Minneapolis, MN 55455

Scanning tunneling microscopy (STM) and atomic force microscopy (AFM) are being used extensively in investigations of surface chemistry in real space and time and in a wide range of environments (vacuum, air, and liquids). The study of molecular adsorbates[1] using scanned probe techniques generally requires an atomically flat substrate in order to resolve atomic and molecular features of the adsorbate. Highly-oriented pyrolytic graphite, HOPG, which is readily cleaved to provide an atomically flat surface, has been used extensively in the past as a substrate for STM studies. Despite the advantage of ease of surface preparation, many molecular adsorbates are weakly physisorbed to HOPG and are prone to tip-induced surface translations, making them difficult to image by scanned probe techniques.

We have recently used a technique developed by Hsu and Cowley[2] for preparing atomically flat Au surfaces, which appears particularly promising as a conductive substrate for STM investigations of adsorbed, electroactive films of transition metal complexes. This technique involves heating a Au wire in a H_2/O_2 flame to form a small molten Au sphere, which is subsequently cooled and annealed to yield atomically flat crystalline surface facets on the order of several tenths of a millimeter in diameter. The following report describes how the quenching and annealing procedure can affect the formation and morphology of Au(111) facets. In particular, we show that elastic and plastic deformations that occur in the Au sphere upon rapid cooling can propagate across the facet to produce highly-ordered surface features with corrugation amplitudes of ~2-12 Å and a periodicity of ~60Å

superimposed on atomically flat terraces. The effects of annealing the Au sphere on this structure and the appearance of the $\sqrt{3}$ x 22 surface reconstruction of Au (111) are discussed.

The structure of the Au surface has been investigated extensively by reflection electron microscopy[3], transmission electron microscopy (TEM)[4], helium atom scattering[5], LEED[6], and x-ray diffraction[7]. Several research groups have characterized the Au(111) surface by STM. In vacuum studies, Kaiser and Jaklevic[8] reported large area topographic images of Au while Hallmark et. al.[9] first reported atomic corrugations on the Au(111) surface. Stacking fault dislocations and reconstructions of the Au(111) surface have been studied with atomic resolution[10, 11]. In addition, the nucleation and growth of various metals on Au(111) has been studied by several groups[12] as well as tip-induced surface modifications[13,14]. The topography of Au(111) in organic solvents has been investigated by Haiss et. al.[15] and Sass et. al.[16]. Electrochemical studies on Au(111) by Wiechers et. al.[17] and Trevor et. al.[18] have shown that the surface roughens and forms a layer of oxide during potential cycling. A recent and detailed STM/electrochemical investigation by Weaver et. al.[19] demonstrates the capability to observe potential-dependent reconstructions of the Au(110) surface. The following work adds to the body of knowledge on Au surfaces by investigating the effect of annealing and quenching ton the formation of smooth and regular Au(111) facets designed to be used as a substrate for the study of molecular adsorbates.

Experimental

Au wire (0.1 mm diameter, 99.999% purity) was obtained from Aesar/Johnson Matthey and cleaned with methanol, acetone and water. Au spheres were formed by heating one end of the wire in a H_2/O_2 flame until red hot and molten. A ~1 mm diameter

sphere is formed at the end of the wire upon cooling. The size of facets on this substrate, which are readily observed under a low power optical microscope, can be markedly increased by annealing the Au sphere in a cooler region of the H_2/O_2 flame. The Au sphere was oriented in a home-built specimen holder so as to expose a facet for STM studies.

Experiments were performed in air using a Nanoscope II (Digital Instruments Inc.) STM. Images were recorded in the constant current mode using the bias voltages and tunneling currents reported in the figure captions. STM tips were prepared by mechanically cutting Pt-Rh (80-20%) wire. Images are typically low-pass filtered to reduce noise.

Results and Discussion

Fig. 1 shows an 1860 nm x 1860 nm region of a Au(111) facet on a well-annealed Au sphere formed by the above described procedure. The facet is characterized by large atomically smooth triangular shaped terraces which extend for several thousands of nanometers on edge. The height of monoatomic steps at the terrace edge is 2.4 ± 0.1 Å, which is the atomic lattice spacing in Au. Several defect lines in the lower half of the image cross the triangular terrace but do not disrupt its macroscopic structure. Fig. 2 is a high resolution image of an Au(111) facet showing the hexagonal arrangement of Au atoms with an interatomic spacing of 3.0 Å, slightly larger the accepted value of 2.88 Å. The hexagonal packing is characteristic of the unreconstructed Au(111) surface.

Figure 3 shows a 80 nm x 80 nm image of the $\sqrt{3}$ x 22 reconstruction of Au(111) on a well-annealed facet. Reconstructions on the (100) surfaces of Pt and Au as well as the (111) face of Au are the result of a hexagonal surface layer of atoms which overlays the bulk cubic structure[5,6b,20]. The reconstruction lines have been attributed to the transition between the fcc and hcp stacking domains in the topmost layer of Au atoms. These stacking faults are the result of a unidirectional contraction of the topmost Au layer with

respect to the lower layers resulting in long-range elastic strain in the reconstructed areas. The misfit between the hexagonal top layer and bulk cubic structure produces a small vertical displacement of the atoms in the top layer.

The reconstruction shown in Fig. 3, known as the "herringbone" reconstruction because the reconstruction lines bend at $\pm 120^{o}$ with respect to one another in a zigzag fashion, has been observed by other researchers in vacuum with both high resolution TEM[21] and STM[12d,11]. Both the herringbone pattern and straight reconstruction lines were routinely observed on well annealed Au(111) samples. As indicated in a recent STM study[11], the fcc region in Fig. 3 corresponds to the apparent minimum (dark region) separating two broad transition regions (bright rows). A second local minimum, in the center of the bright rows, corresponds to hcp domains. The corrugation amplitude between the wide minima and maxima is ~0.2 Å, while the corrugation amplitude between the narrower minima and wide maxima is ~0.03 Å. The distance between adjacent broad minima in Fig. 3 is 65 - 75 Å, in agreement with values reported in previous STM[11] and He diffraction measurements in vacuum[5].

In addition to the $\sqrt{3} \times 22$ reconstruction, which is observed only on well-annealed surfaces, we have observed unusually large corrugations on (111) surface of Au spheres which have not been annealed. In particular, Au spheres which are melted and then cooled rapidly in air form macroscopic ripples upon solidification which propagate out from the region where the wire meets the sphere. These macroscopic surface ripples, which are readily observed in a light microscope, tend to propagate around individual facets on the substrate. However, STM images of these well-defined (111) facets indicate that elastic stresses in the sphere can propagate though the crystal causing the (111) surface to buckle along reconstruction lines.

Fig. 4(a) shows a 180 nm x 180 nm area of a (111) facet which is surrounded by macroscopic ripples. The surface is covered with highly periodic rows (oriented from the

top left to the bottom right corner of the image) with a spacing of ~50 Å between the rows. Corrugation amplitudes are on the order of 2.1 Å, significantly larger than those of the normal reconstruction (~0.2 Å in Fig. 3). In addition, the previous images of the normal reconstruction shown in Fig. 3 show rows with an approximately uniform height along the length of the row, while those in Fig. 4(a) have regions along the row which bulge upwards creating local maxima.

Fig. (4b) shows a 150 nm x 150 nm image of a (111) facet on a different Au sphere. The triangular facets are covered with rows whose spacing is ~60 Å, but with a corrugation amplitude of 5-12 Å, much larger than seen in previous studies of Au. Once again, the height of a row can vary along the length of the row and can have local maxima such as those in Fig. (4a). The rows pass from one terrace to another without any disruption in structure, as seen in Fig. 4(b). Fig. 4(c) shows another (111) triangular facet on which rows with large corrugations are evident. Again, the spacing between the rows is ~50 Å and the corrugation amplitude ranges from 2.1 Å.to 4.0 Å. In this image, there is an increase in the height of the rows along the edge of the terrace and decrease on either side of the edge. Fig. 4(d) is a surface plot of the area in Fig. 4(a) emphasizing the corrugation amplitude of these rows. Fig. 5 compares the topographic profile of the normal $\sqrt{3}$ x 22 reconstructions on Au(111), shown in Fig. 3, with that of the rows with the large corrugation amplitudes shown in Fig. 4(b). Even though the periodicity of the rows is approximately the same, the difference in the corrugation amplitude between the two is ~35x (note the differences in the y axis scale).

Previous high resolution TEM studies[22] of the Au(111) surface indicate that this surface can undergo inhomogeneous plastic and elastic deformations giving rise to a buckled surface structure when a large positive tangential surface pressure is applied. Corrugation amplitudes in the buckled region (as measured from edge-on micrographs) were found to be as large as 15 Å. The electronic configuration of the Au atoms[23], in

particular, the inherent cohesive forces resulting from interactions of the 6sp and 5d electrons, has been used as a basis to explain the buckling which can occur on Au(111) surfaces. The termination of the bulk lattice at the surface creates an imbalance in these electronic forces (see refs. 22 and 23), resulting in a positive tangential surface pressure that can be relieved by the observed buckling of the surface. However, in the present studies, the tangential surface pressure most probably results from macroscopic stresses throughout the Au sphere that arise during rapid solidification. This view is supported by the fact that the large corrugated rows are not observed on carefully annealed samples.

Moritz and Wolf[24] have attributed distortions on Au surfaces to rotation of the (111) microfacets with respect to one another. The processes which contributed to the surface distortion were thought to involve several atomic layers. No evidence was found in the present study to support this mechanism. Giant corrugations have been documented on HOPG and are believed to involve a rotational mismatch of the top graphite layer with respect to the lower layers[25].

It is interesting to note that the periodicity of the large corrugations (50 - 65Å) is similar to that of the spacing between maxima and minima observed on the $\sqrt{3}$ x 22 Au surface (64Å). Whether this finding is coincidental or is due to a transition between the two structures upon annealing is not known and is currently being investigated.

Conclusions

This work shows that the Au(111) facets formed on Au sphere can exhibit not only the normal $\sqrt{3}$ x 22 reconstruction with corrugation amplitudes in the range of ~0.2 Å, but can also exhibit rows with anomalously high corrugation amplitudes of ~2-12 Å. Although the mechanism by which these rows are produced is not full understood, it is postulated that elastic stresses in the Au sphere can propagate through the crystal the Au(111) surface

to buckle. Work is in progress to determine the conditions during the solidification and annealing process which lead to these highly corrugated surface structures.

Acknowledgments

The author gratefully acknowledges The Electrochemical Society for support of this work in the form of financial support under the Edward G. Weston Fellowship Award for the summer of 1991. Acknowledgement is made to the Office of Naval Research for the continuation of this research. In addition, the author extends special thanks to Dr. Joachim Schott and Prof. Henry S. White for valuable discussions and insights during the course of this work and to Sidhar Rao for technical assistance.

References

1. (a) P.H. Lippel, R.J. Wilson, M.D. Miller, Ch. Woll, and S. Chiang, *Phys. Rev. Lett.*, **62**, 171, (1989) (b) B.C. Schardt, S. Yau, and F. Rinaldi, *Science*, **243**, 1050 (1989) (c) H. Ohtani, R.J. Wilson, S. Chiang, and C.M. Mate, *Phys. Rev. Lett.*, 60, 2398 (1988) (d) J.S. Foster and J.E. Frommer, *Nature*, **333**, 542 (1988) (e) G.C. McGonigal, R.H. Berhardt, and D.J. Thomson, *Appl. Phys Lett.*, **57**, 28 (1990) (f) T. Sleator and R. Tycho, *Phys. Rev. Lett.*, **60**, 1418 (1988) (g) S.R. Snyder, H.S. White, S. Lopez, and H.D. Abruna, *J. Am. Chem. Soc.*, **112**, 1333 (1990) (h) S. Gould, O. Marti, B. Drake, L. Hellemans, C.E. Bracker, P.K. Hansma, N.L. Keder, M.M. Eddy, and G.D. Stucky, *Nature*, **332**, 332 (1988) (i) C.M. Mate, M.R. Lorenz, and V.J. Novotny, *J. Chem. Phys.*, **90(12)**, 7550 (1989).

2. T. Hsu and J.M. Cowley, *Ultramicroscopy*, **11**, 125 (1983).

3. (a) Y. Uchida, G. Lehmpfuhl, and J. Jager, *Ultramicroscopy*, **15**, 119 (1984) (b) G. Lehmpfuhl and Y. Uchida, *Surf. Sci.*, **235**, 295 (1990).

4. (a) G. Lehmpfuhl and Y. Uchida, *Ultramicroscopy*, **4**, 275 (1979) (b) S. Iijima, *Ultramicroscopy*, **6**, 41 (1981).

5. U. Harten, A.M. Lahee, J.P. Toennies, and Ch. Woll, *Phys. Rev. Lett.*, **54**, 2619 (1985).

6. (a) W. Moritz and D. Wolf, *Surf. Sci.*, **88**, L29 (1979) (b) M.A. Van Hove, R.J. Koestner, P.C. Stair, J.P. Biberian, L.L. Kesmodel, I. Bartos, and G.A. Somorjai, *Surf. Sci.*, **103**, 189 and 218 (1981).

7. E. Vlieg, I.K. Robinson, and K. Kern, *Surf. Sci.*, **233**, 248 (1990).

8. W.J. Kaiser and R.C. Jaklevic, *Surf. Sci.*, **182**, L227 (1987).

9. V.M. Hallmark, S. Chiang, J.F. Rabolt, J.D. Swalen, and R.J. Wilson, *Phys. Rev. Lett.*, **59(25)**, 2879 (1987).

10. Ch. Woll, S. Chiang, R.J. Wilson, and P.H. Lippel, *Phys. Rev. B*, **39(11)**, 7988 (1989).

11. J.V. Barth, H. Brune, G. Ertl, and R.J. Behm, *Phys. Rev. B.*, **42(15)**, 9307 (1990).

12. (a) O.M. Magnussen, J. Hotlos, R.J. Nichols, D.M. Kolb, and R.J. Behm, *Phys. Rev. Lett.*, **64(24)**, 2929 (1990) (b) A. Brodde, St. Tosch, and H. Neddermeyer, *J. of Microscopy*, **152**, 441 (1988) (c) M.M. Dovek, C.A. Lang, J. Nogami, and C.F. Quate, *Phys. Rev. B.*, **40(17)**, 11973 (1989) (d) D.D. Chambliss and R.J. Wilson, *J. Vac. Sci. Technol. B*, **9(2)**, 928 (1991) (e) D.D. Chambliss, R.J. Wilson, and S. Chiang, J. Vac. Sci. Technol. B, **9(2)**, 933 (1991).

13. H.J. Mamin, P.H. Guethner, and D. Rugar, *Phys. Rev. Lett.*, **65(19)**, 2418 (1990).

14. L. Nagahara, S.M. Lindsay, T. Thundat, and U. Knipping, *J. Microsc.*, **152**, 145 (1988).

15. W. Haiss, D. Lackey and J.K. Sass, submitted to *J. Chem. Phys.*.

16. J.K. Sass, J.K. Gimzewski, W. Haiss, K.H. Besocke and D. Lackey, submitted to *J. Phys.: Condens. Matter 1*.

17. J. Wiechers, T. Twomey, D.M. Kolb, and R.J. Behm, *J. Electroanal. Chem.*, **248**, 451 (1988).

18. D.J. Trevor, C.E.D. Chidsey, and D.N. Loiacono, *Phys. Rev. Lett.*, **62(8)**, 929 (1989).

19. X. Gao, A. Hamelin, and M.J. Weaver, *Phys. Rev. Lett.*, **67(5)**, 618 (1991).

20. K. Takayanagi and K. Yagi, *Trans. Jpn. Inst. Met.*, **24**, 337 (1983).

21. Y. Tanishiro, H. Kanamori, K. Takayanagi, K. Yagi, and G. Honjo, *Surf. Sci.*, **111**, 395 (1981) (b) J.C. Heyraud and J.J. Metois, *Surf. Sci.*, **100**, 519 (1980).

22. (a) D.J. Smith and L.D. Marks, *Ultramicroscopy*, **16**, 101 (1985) (b) L.D. Marks, V. Heine, and D.J. Smith, *Phys. Rev. Lett.*, **52(8)**, 656 (1984).

23. (a) V. Heine and L.D. Marks, *Surf. Sci.*, **165**, 65 (1986) (b) R.J. Needs and M. Mansfield, *J. Phys.: Condens. Matter* **1**, 7555 (1989) (c) D. G. Pettifor, *J. Phys. F: Metal Phys.*, **8(2)**, 219 (1978).

24. W. Moritz and D. Wolf, *Bull. Am. Phys. Soc.*, **30**, 460 (1985).

25. (a) S.R. Snyder, M.S. Thesis, University of Minnesota (1990) (b) M. Kuwabara, D.R. Clarke, and D.A. Smith, *Appl. Phys. Lett.*, **56(24)**, 2396 (1990) (c) C. Liu, H. Chang, and A.J. Bard, *Langmuir*, **7(6)**, 1138 (1991).

Figure Captions

Figure 1. STM image of a well-annealed Au(111) facet. Sample bias voltage, V_t, = 50.0 mV and tunneling current, I_t, = 3.3 nA.

Figure 2. High resolution STM image showing atomically corrugation on an Au(111) facet. (V_t = 10.4 mV; I_t = 14.9 nA.)

Figure 3. STM image of the $\sqrt{3}$ x 22 reconstruction of Au(111). (V_t = -80.6 mV; I_t = 1.8 nA.)

Figure 4. STM images of the large-amplitude corrugated (111) surface of rapidly quenched Au. (a) Image showing a Au(111) facet covered with rows with periodicity ~50 Å and corrugation amplitude ~2.1 Å. (V_t = -174.9 mV; I_t = 2.3 nA.); (b) Image of a microfaceted region covered with rows of corrugation amplitude ~5-12Å and periodicity ~60 Å.. The rows continue from one microfacet to another. (V_t = -131.5 mV; I_t = 0.1 nA.); (c) Image of the apex of a triangular terrace covered by rows with a periodicity of ~50 Å and corrugation amplitude ranging from ~2.1 Å to ~4.0 Å. (V_t = 174.9 mV; I_t = 3.4 nA.); (d) Surface plot of the area imaged in Fig. 4(b). In this section of the sample, the corrugation amplitude is ~4.0 and the spacing is ~66 Å. (V_t = -131.5 mV; I_t = 0.1 nA.)

Figure 5. Lines profiles across the (a) $\sqrt{3}$ x 22 reconstruction of Au(111) in Fig. 2, and (b) the large corrugated rows shown in Fig. 3(b). Note change in scale of the corrugation amplitude.

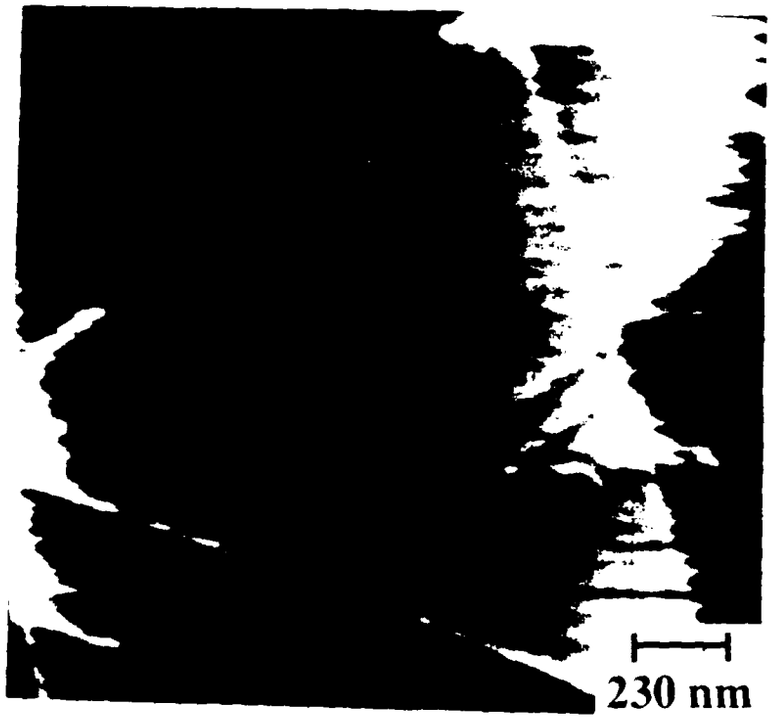
230 nm

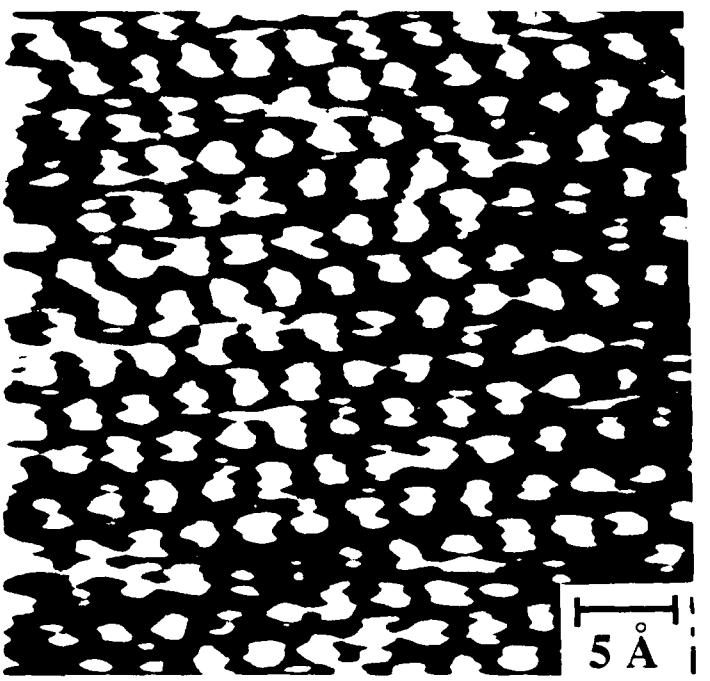
5 Å

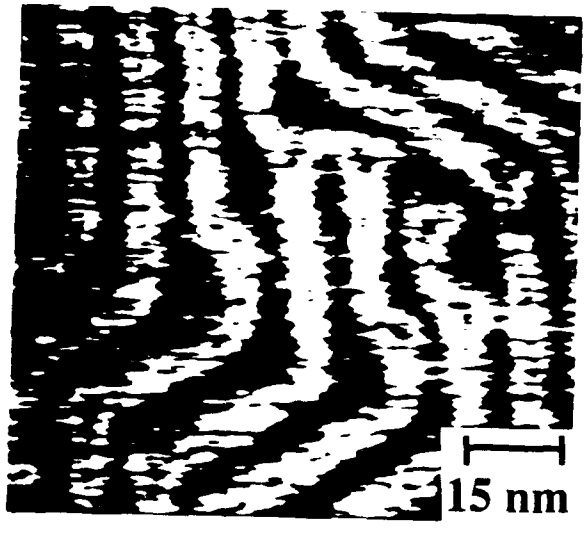
15 nm

(a)

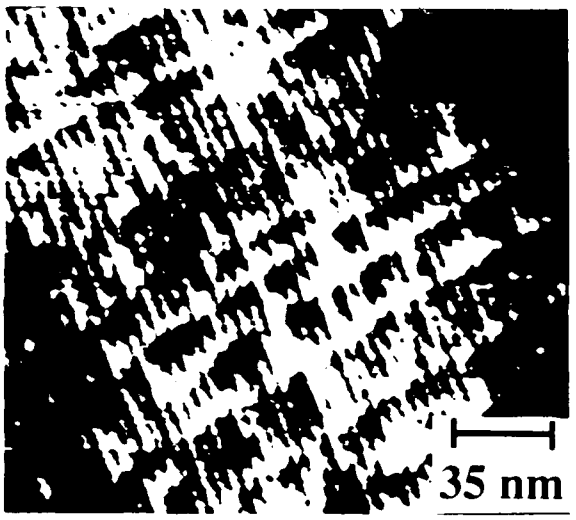

(b)

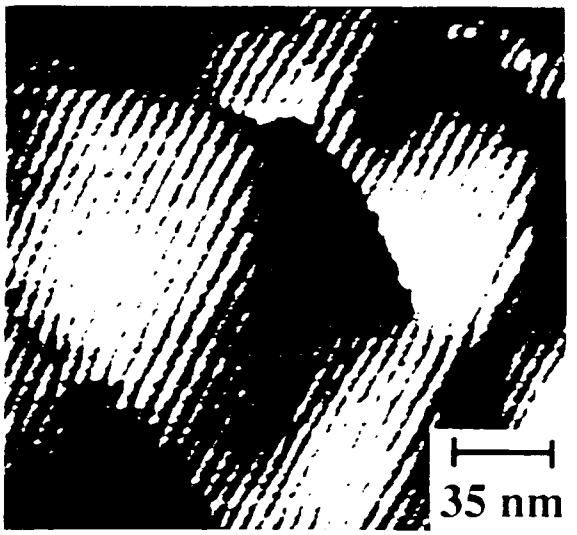

(c)

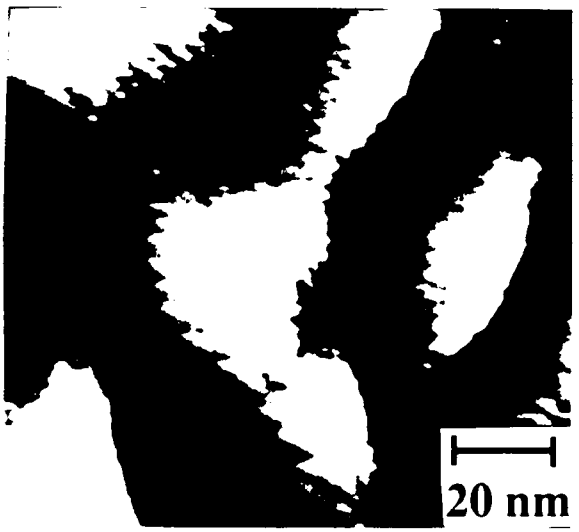

(d)

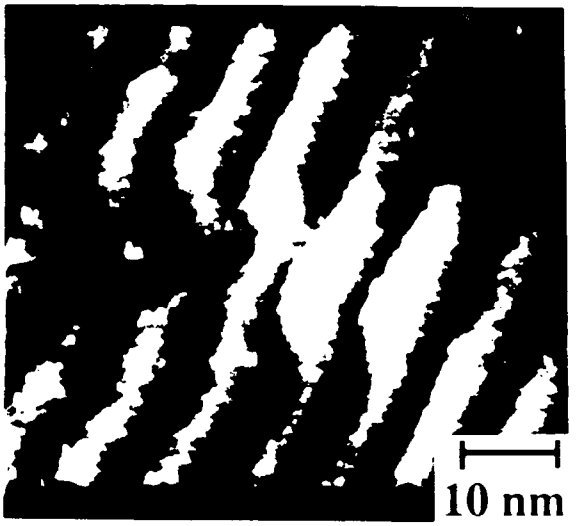

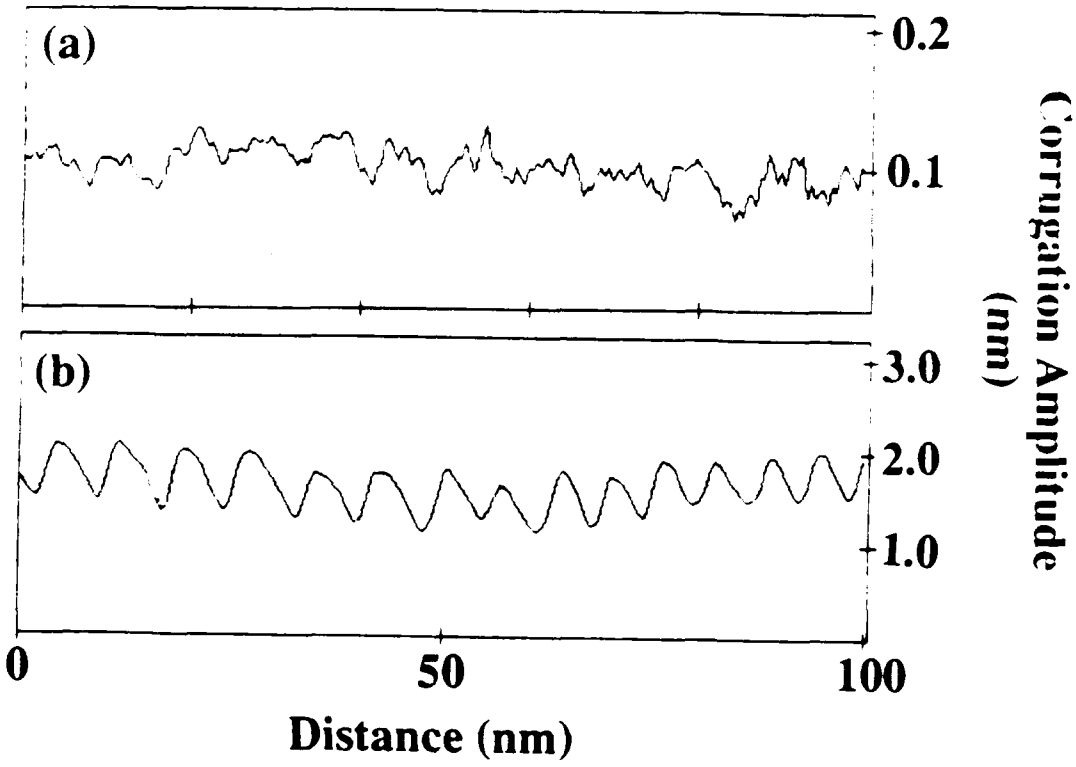
(a)
0.2
0.1
(b)
3.0
2.0
1.0
Corrugation Amplitude (nm)
0
50
100
Distance (nm)